NATIONAL ADVISORY COMMITTEE FOR AERONAUTICS

TECHNICAL NOTE 4247

STUDY OF GROUND-REACTION FORCES MEASURED DURING LANDING IMPACTS OF A LARGE AIRPLANE

By Albert W. Hall, Richard H. Sawyer, and James M. McKay

Langley Aeronautical Laboratory
Langley Field, Va.

Washington
May, 1958

NATIONAL ADVISORY COMMITTEE FOR AERONAUTIC

1Y

TECHNICAL NOTE 4247

STUDY OF GROUND-REACTION FORCES MEASURED DURING LANDING IMPACTS OF A LARGE AIRPLANE[1]

By Albert W. Hall, Richard H. Sawyer, and James M. McKay

SUMMARY

Some results are presented of tests conducted on a large bomber-type airplane to determine the ground-reaction forces imposed on the main landing gear under actual landing conditions. The data were obtained from 30 landings made at vertical velocities up to 8.4 feet per second and at forward ground speeds from 81.0 to 119.5 knots on both wet and dry concrete runways.

The vertical force on the landing gear truck at which the oleopneumatic shock strut began to compress varied over a wide range. There appeared to be no relation between this breakout force and any other force or condition of the impact.

The computed variation of maximum vertical force with vertical velocity agreed reasonably well with the experimental results.

Frequently there was an unequal division of the vertical force on the two wheels of a truck, which resulted in unsymmetrical drag forces particularly during the time when one wheel had spun up and the other was still in the process of spinning up.

The mean value of coefficient of friction for the dry runway varied from 0.40 at the beginning of spin-up to a maximum value of 0.72 at a slip ratio of 0.13. The mean value of coefficient of friction for the wet runway varied from 0.20 at the beginning of spin-up to a maximum value of 0.41 at a slip ratio of 0.07.

In the low vertical-force range, the side force varied with drift angle and vertical force. At high vertical forces, side force varied primarily with drift angle and further increase of vertical force had little effect on side force at a given drift angle.

---

[1]Supersedes NACA Research Memorandum L55E12c by Richard H. Sawyer, Albert W. Hall, and James M. McKay, 1955.

INTRODUCTION

The need for a more accurate knowledge of the loads imposed on the landing gear has become increasingly important in the structural design of airplanes. Prediction of dynamic structural loads on the landing gear and on the airplane is possible by a number of methods of dynamic analysis which permit reasonable accuracy in the calculation of the dynamic response when the forcing functions are known. In order to obtain information on these forcing functions, the ground forces imposed on the main landing gear of a large airplane under actual landing conditions were measured. The main landing gear of this airplane was equipped with strain gages and linear and angular accelerometers in order to measure ground-reaction forces during landing impacts. The airplane was equipped with various types of special and standard flight instruments to determine the landing-impact and landing-approach conditions.

The results presented in this report include the variation of vertical force with vertical velocity, the variation of the coefficient of friction with slip ratio during the spin-up process for both wet and dry concrete surfaces, and the side-force variation with drift angle and vertical force.

SYMBOLS

F_h	drag force (forward and rearward direction), lb
F_s	side force, lb
F_v	vertical force, lb
I_θ	moment of inertia of wheel about axle, 33.5 slug-ft^2
K_s	tire lateral deflection parameter, y/F_s, ft/lb
M	axle bending moment; used with subscripts h and v to denote moments in horizontal and vertical planes, respectively
r_d	distance from axle to ground (Undeflected tire radius minus Tire deflection), ft

T	torque, $F_h r_d$
V_v	vertical velocity of landing gear, fps
W	gross weight of airplane, lb
y	lateral shift of vertical-force center of pressure due to side force, ft
$\ddot{\theta}$	angular acceleration of wheel, radians/sec^2
μ	coefficient of friction, $\frac{F_h}{F_v}$

Subscripts:

1	axle strain-gage station 1
2	axle strain-gage station 2
max	maximum

LANDING GEAR

The airplane used in the investigation (fig. 1) had a conventional tricycle landing gear with dual wheels on the main and nose gear, each wheel having a separate axle. The general arrangement of one of the main-landing-gear trucks is shown in figure 2 with one wheel removed. (The term "truck" is used in this report when a pair of wheels is referred to as a unit.) The main landing gear had smooth-contour tires 56 inches in diameter, inflated to a pressure of 75 pounds per square inch for the light condition and 90 pounds per square inch for the heavy condition. The tire treads used in the tests on the dry runway were diamond, oval, rib, and an interlocking cross-type pattern similar to the oval and diamond. The rib-type treads were installed at the time of the tests on the wet runway. Each main wheel including the tire, tube, brake, and instrumentation weighed approximately 700 pounds. The main-landing-gear oleopneumatic shock strut had a stroke of 12 inches and was normally inflated with air so that it extended about 2 inches from the bottomed position (compressed) while on the ground (approximately 700 pounds per square inch for the light-weight condition).

INSTRUMENTATION

The quantities measured for the purpose of defining both the landing-approach conditions and the impact and spin-up conditions are as follows:

Approach	Impact
Center-of-gravity acceleration	Wheel vertical reaction
Airspeed	Wheel drag reaction
Pitch attitude	Wheel side reaction
Pitching velocity	Vertical velocity
Roll attitude	Tire deflection
Rolling velocity	Wheel rotational velocity
Yaw angle	Shock-strut displacement
Yawing velocity	Wheel motion pictures
Drift angle	
Control-surface deflections	

The location of some of the instrumentation is shown in figure 2. The strain-gage locations are shown in more detail in figure 3 which represents a vertical cross section of the axle structure. The strain gages were also located in the same lateral position in the horizontal plane. The strain-gage bridges located in the vertical plane measure the bending moment at stations 1 and 2 due to the vertical component of force applied at the axle and the moment due to side force. Similarly, the strain gages in the horizontal plane measure the bending moments due to the horizontal component of force at the axle and the moment contributed by the side force when it is out of the vertical plane. The linear accelerometers mounted on the outer brake shoe were used to determine the horizontal and vertical inertia forces. Angular accelerometers mounted inside the outboard wheels were used to measure angular acceleration of the outboard wheels. The mean tire deflections for each pair of wheels were obtained by means of a slide-wire position recorder connected to a trailing arm which was mounted between the wheels. The vertical velocity of each truck was measured by an electromagnetic generator attached to the trailing arm, similar to the arrangement described in reference 1. The angular velocity of each wheel was measured by a tachometer mounted on the outer brake shoe and geared to the wheel. The instruments used to measure the approach conditions presented in the foregoing table, except for drift angle, were standard NACA flight recording instruments. The drift angle was measured by means of a 16-millimeter motion-picture camera mounted on the bottom of the airplane fuselage to photograph the runway directly below the camera. The shutter

speed was slow enough to cause spots and irregularities on the runway to appear as streaks on the film when the airplane was in motion. The angle of these streaks relative to the edge of the picture was a measure of drift angle. An NACA 0.01-second timer was used to put a time signal on each recorder and on the edge of the 16-millimeter motion-picture film. An attempt was made wherever possible to minimize instrument response errors.

TEST PROGRAM

The test program consisted of 30 landings made by a large bomber-type airplane at vertical velocities ranging up to 8.4 feet per second and forward ground speeds at contact from 81.0 to 119.5 knots. All of the landings were made on concrete runways (numbers 7 and 25) at Langley Air Force Base, Va. Twenty-four landings were made with the airplane gross weight between 95,000 and 100,000 pounds. Of these 24 landings, 18 were made on dry concrete and 6 were made on a runway wetted down by fire hoses to simulate a heavy rain. Six landings were made on dry concrete with the airplane gross weight about 120,000 pounds. Many of the landings consisted of several separate impacts on the same truck. The test conditions are presented in detail in tables I and II.

DATA REDUCTION

The main-landing-gear axle structure (fig. 3) was used as a strain-gage balance to measure vertical, drag, and side forces on the axle. The accuracy of the strain-gage balance was poor in the low range (up to about 4,000 pounds) and under certain combined forces due in part to the nonhomogeneous axle and housing structure on which the strain gages were mounted.

The following relationships can be seen from figure 3 which shows a vertical cross section of the axle structure and the components of forces and moments in the vertical plane:

$$M_{V,1} = F_V\left[A + (B - y)\right] - F_S r_d$$

$$M_{V,2} = F_V(B - y) - F_S r_d$$

Substituting gives

$$M_{v,1} = F_v A + M_{v,2}$$

$$F_v = \frac{M_{v,1} - M_{v,2}}{A}$$

Similarly, in a horizontal plane

$$F_h = \frac{M_{h,1} - M_{h,2}}{A}$$

Thus, the magnitude of a force, regardless of its lateral position, could be determined by measuring the moment at two positions located a known distance apart. As a result of interaction (effects of vertical forces on horizontal strain gages and vice versa) and misalinement of the strain gages, the final equations for measuring axle forces had the form:

$$F_v = C_{v,1}M_{v,1} + C_{v,2}M_{v,2} + C_{v,3}M_{h,1} + C_{v,4}M_{h,2}$$

$$F_h = C_{h,1}M_{v,1} + C_{h,2}M_{v,2} + C_{h,3}M_{h,1} + C_{h,4}M_{h,2}$$

where $C_{v(1,2,3,4)}$ and $C_{h(1,2,3,4)}$ were constants determined from calibration loadings.

The ground-reaction forces, both vertical and drag, were obtained by adding inertia corrections to the axle forces. The inertia term was the product of the mass outboard of the strain-gage stations (wheel, brakes, instruments, etc.) and the vertical or horizontal acceleration of the center of this mass. The accelerometers used to measure the vertical and horizontal accelerations could not be located at the mass center but were located as close as possible to the mass center on the vertical axis and horizontal axis, respectively. Owing to the frequency-response characteristics of the instrumentation, the inertia corrections are in error when the force is changing very rapidly, such as occurs in some cases of springback when the drag force goes from a large positive (rearward) value to some negative (forward) value.

Because of the nature of the axle and housing structure it was virtually impossible to locate strain gages which were primarily sensitive to side force. It became necessary to evaluate the side force F_s for each wheel by means of the bending moment $M_{v,2}$ produced by the side

force and the vertical force on the axle. From figure 3 the following relations are found:

$$M_{v,2} = F_v(B - y) - F_s r_d$$

where by definition of K_s

$$y = K_s F_s$$

Therefore,

$$M_{v,2} = F_v B - F_s(\dot{r}_d + F_v K_s)$$

or

$$F_s = \frac{F_v B - M_{v,2}}{r_d + K_s F_v}$$

The order of magnitude of K_s was determined from results presented in reference 2. The value of the product $K_s F_v$ was small in comparison with the value of r_d so that the actual value of K_s was not critical. The side-force results are believed to indicate qualitatively the nature of side-force buildup and variation with drift angle and vertical force.

The drag force F_h was determined from strain-gage measurements for all of the wheels and also from angular-accelerometer measurements for the outboard wheels of each truck. The angular-accelerometer method involved the use of the expression $T = F_h r_d = I_\theta \ddot{\theta}$. This expression neglects the torque produced by the vertical force F_v acting through some forward or rearward displacement relative to the axle center line. Although the forces are of the same order of magnitude $F_h = \mu F_v$, the moment arm of the vertical force is a small percentage of the moment arm of the drag force. This method of measuring F_h is similar to that used in reference 3 where the agreement with simultaneous dynamometer measurements was good.

On the basis of calibration loading data and of comparisons of F_h determined from both the strain-gage and angular-accelerometer measurements for the outboard wheels, the drag-force data determined from the angular-accelerometer method were felt to be the most reliable. The strain-gage drag-force data for the outboard wheels were generally in good agreement with the angular-accelerometer drag-force data but the

strain-gage drag-force data for the inboard wheels were considered unreliable in magnitude but usable to indicate the shape of the drag-force time history for the impact. In presenting the coefficient-of-friction data, only F_h obtained by the angular-accelerometer method was used.

RESULTS AND DISCUSSION

The approach conditions just prior to ground contact are given in tables I and II. The maximum roll attitude was 2.9° (left wing down) and all of the landings except one had first contact of the main gear on the left truck. For the landing in which the right truck made first contact the roll attitude was 1.2° (right wing down). The pitch attitude at contact covered a range from 0.1°, at which the nose wheels contacted first, to 8.8°, at which the tail skid hit first. The airplane lift at contact is presented in table II as center-of-gravity normal acceleration just prior to the time that the first wheel made contact. For the 30 landings the lift at contact varied from approximately 94 to 111 percent of the airplane weight. There appeared to be no consistent effect of vertical velocity on lift at contact.

Typical samples of time histories of ground-reaction forces and of the corresponding wheel angular velocities for several impacts are given in figure 4. These samples were selected as being typical of the various conditions encountered during the test program. These conditions are discussed in detail in subsequent sections of this report. Some of the impacts presented in figure 4 begin at values of time other than zero and this indicates that for this landing the particular impact shown occurred after the first truck touched the runway, since zero time was taken to coincide with the time of the first truck to contact. Instrument failures during the tests resulted in the loss of some data; for example, in figure 4(b) part of the drag time history by the angular-accelerometer method is missing, and in figure 4(d) both drag time histories are missing for the left outboard wheel.

Vertical Force

Figure 4(a) illustrates an unequal division of vertical force F_V between two wheels of the same truck, which is a result of one or more factors, such as airplane roll attitude, landing-gear inclination (in roll plane) due to wing bending, or differences in tire diameter. During this particular landing, the value of F_V was low and only the inboard wheel spun up during the first impact while the outboard wheel partially spun up and then spun up completely during the second impact. This landing, in which one wheel completed its spin-up during the second

impact, was typical of a number of landings encountered in this test program. The impact shown in figure 4(c) also shows an unequal division of F_V between the two wheels.

The point at which the oleo shock strut begins to compress is indicated by ticks on the vertical-force time histories of figures 4(b) to 4(f). For the impacts shown in figure 4(a) the shock strut did not compress during either impact. The value of F_V at which the shock strut begins to compress (breakout force) is given in table I for all of the impacts in which the shock strut compressed. This value of F_V is the total vertical force on the truck (both wheels) at the instant the shock strut breaks free and begins to compress. From table I it may be seen that the values of breakout force vary from 9,000 to 45,500 pounds. An attempt to relate the breakout force to initial preload and binding of the strut due to drag force, vertical force, unsymmetrical vertical force, etc., was not successful.

The effect of the sudden release of the shock strut on the vertical-force time history is to decrease the rate of vertical-force buildup and in some cases even to reduce the vertical force for a short time (figs. 4(b) to 4(f)).

The variation of maximum vertical force on the truck with vertical velocity (fig. 5) was calculated by a numerical integration method similar to that discussed in reference 4. In order to simplify the calculations, a symmetrical impact was assumed, the airplane was assumed to be rigid, the lower or unsprung mass was neglected, the pneumatic force was assumed to be constant, and a linear approximation of the actual static-force-deflection characteristics of the tire was used. The physical characteristics of the shock strut of the airplane used in these tests were used in these calculations, the airplane weight was taken as 100,000 pounds, and the lift was assumed equal to the weight. One curve was calculated by assuming zero breakout force and a constant metering-pin area equal to that part of the pin in action at the beginning of the stroke. Another curve was calculated by using the constant metering-pin area, a shock-strut breakout force of 24,000 pounds, and the static tire characteristics from zero to 24,000 pounds. As a point of interest it may be seen that the curve for zero breakout force can be transposed to the curve for 24,000-pound breakout force by moving each point up 24,000 pounds and over 1.6 feet per second. Thus, a curve for zero breakout force may be determined with the aid of charts presented in reference 4 and then a curve for a given breakout force can be quickly determined.

A third curve was calculated by using a 24,000-pound breakout force and the actual metering-pin-area variation with strut stroke. At a

value of V_V just beyond a vertical velocity of 4.3 feet per second, the stroke is sufficient to move the constant area portion of the metering pin out of the orifice plane, and the effect of the decreasing metering-pin area with stroke becomes apparent in the reduction of maximum force at a given vertical velocity.

Figure 6 shows the maximum vertical force on a truck divided by one-half of the gross weight plotted against the corresponding vertical velocities for each impact for both the light-weight and heavy-weight conditions. For comparison, the calculated curve for a breakout force of 24,000 pounds and the actual metering-pin-area variation is also shown. The trend of the measured values appears to be similar to the trend of those calculated but there is considerable scatter in the measured values. This scatter does not appear to be related to the different values of the breakout force corresponding to the various points. Furthermore, an attempt to correct the measured values to those corresponding to a symmetrical landing with lift equal to the airplane weight and zero rolling velocity on the basis of a simplified theory for a rigid airplane did not result in any reduction of the scatter. An attempt to relate the scatter to the effect of lift, attitude, and rolling velocity by means of an empirical analysis was equally unsuccessful. Because of the limited amount of data and the scatter present, no effect of increasing the weight approximately 20 percent could be determined.

The relation between the vertical force at the time of maximum drag force and the maximum vertical force for each impact is presented in figure 7. The solid line represents the locus of points at which maximum vertical and drag forces occur simultaneously. In the range of maximum vertical force below 30,000 pounds there are a number of points on this line. In the higher range of maximum vertical force, it appears that there might be a possibility that the maximum vertical and drag forces would not occur simultaneously; however, the limited data available in the high load range preclude any definite conclusions.

Drag Force

Typical time histories of drag force, which are presented in figure 4 for a range of vertical velocities, show that in most cases the drag force builds up to a maximum value as the wheel comes up to 80 or 90 percent of the free rolling speed. The drag force then drops rapidly to zero and then negative as the wheel comes up to and then overshoots the free rolling speed. In some cases, such as that shown in figure 4(c) for the left inboard wheel, the drag force starts to build up, then to decrease, and then to increase again. This type of variation was found in several other impacts, not shown here, in which the drag force near the middle of the spin-up period was greater than that when the wheel was near 80 or 90 percent of the free rolling speed. Since the changes

in coefficient of friction are small, it appears that these variations in drag force are generally attributable to corresponding vertical-force variations.

The unequal division of vertical force on two wheels of the same truck results in unsymmetrical drag forces, particularly at the time when one wheel has spun up and its drag force has decreased while the other wheel is approaching maximum drag force. This distribution of drag force results in a severe yawing moment about the vertical axis of the truck and the resulting yawing oscillation has been observed in slow-motion pictures of the trucks during impact.

Coefficient of friction.- The variation of coefficient of friction μ with slip ratio is presented in figure 8. The expression slip ratio is defined in the appendix by equation (1). The top curve in figure 8(a) shows the variation of μ with slip ratio for an impact on a dry runway with the vertical velocity at contact equal to 3.85 feet per second. At the instant of contact the angular velocity of the wheel was zero and the slip ratio was 1.0; as the wheel velocity approaches the free rolling velocity, the slip ratio approaches 0. The forces were too small to give reliable values of μ until the slip ratio had decreased to approximately 0.9. As the wheel comes up to free rolling speed, the value of μ gradually increases to a maximum value of 0.73 at a slip ratio of 0.11. The variation from μ_{max} to zero slip ratio is not shown because the drag force dropped so rapidly in this range that the values of μ are unreliable and the slip ratio is difficult to measure accurately in this range. The bottom curve in figure 8(a) is for a comparable impact on a wet runway.

The faired curves from these and other impacts were used in figure 8(b). The envelopes of the curves formed the boundaries shown and the curve within each boundary was the mean curve for each case (wet and dry runway). The point indicating μ_{max} for each case was the mean of the individual values of μ_{max} and of the mean slip ratio at which μ_{max} occurred. The mean value of μ for the dry runway increased gradually from a value of 0.40 near the beginning of spin-up (slip ratio of 0.90) to a maximum value of 0.72 at a slip ratio of 0.13. The mean value of μ for the wet runway varied from 0.20 near the beginning of spin-up to a maximum value of 0.41 at a slip ratio of 0.07.

The differences in the variation of μ among landings is believed to be caused primarily by differences in the condition of the runway surface - for example, for the dry runway the presence of skid marks, oil, dirt, etc., and for the wet runway by these same effects and the amount of water present on the runway.

Computed forces.- Computations of the drag forces during the landing impact were made for one landing condition for comparison with the measured drag forces. Measured vertical forces, approximate measurements of first bending and torsion frequencies of the landing gear, and a two-segment linear approximation to the variation of tire-to-runway friction coefficient with slip ratio shown in figure 8(b) were used in the computation. The procedure is outlined in the appendix. Time histories of the computed ground-reaction drag forces are compared in figure 9 with those of the measured results for the two wheels of a truck. The time variation of the drag force of each wheel is predicted with reasonable accuracy, particularly the difference in the spin-up time of the two wheels which resulted from the unsymmetrical impact.

The ultimate purpose of the tire-to-surface friction measurements is to provide information for use in the study and prediction of landing loads imposed on the aircraft structure. The computations were extended, therefore, to include determination of the dynamic bending moment about the vertical axis at one point in each wheel axle for which strain-gage measurements were available for comparison. The comparisons of the measured and computed axle-bending-moment time histories are shown for the two wheels of the truck in figure 10. Computed static bending moments are included to indicate the extent of the dynamic part of the load in the axle. The computed and experimental axle-load time histories are at least qualitatively similar, although there are some differences in amplitude and phase of the oscillating load. Both computed and experimental results show rather large dynamic loads that arise primarily from excitation of the torsion (yawing) mode of the landing gear by the large and abrupt difference in drag ground-reaction forces on the two wheels, which occurs when one wheel is operating in the region of slip ratios greater than that at which μ_{max} occurred and the other wheel is operating at slip ratios less than that at which μ_{max} occurred. The variation of μ with slip ratio is much greater for the second region than for the first region.

Side Force

Some typical time histories of side force during spin-up are shown in figure 4. The side force builds up gradually during the first part of the spin-up, and, as the wheel approaches the free rolling speed, the side force increases more rapidly to the full value after spin-up. The data of figure 4 and also the data not shown indicate that generally at the time of maximum drag force the side force is about 30 to 50 percent of the maximum value. There were cases where maximum side force and maximum vertical force occurred simultaneously and there were several instances in which maximum drag force and maximum vertical force occurred simultaneously. However, it would appear unlikely that all three forces

would reach their maximum value simultaneously. Figure 4(c) presents data for an impact in which the drift angle was between 4° and 4.5° and a large value of side force is indicated. The side force after spin-up is almost the same for each wheel of the truck while the vertical load is much greater for the outboard wheel; this indicates, for this higher range of F_V, that the side force is dependent on drift angle rather than on vertical load. This fact is more clearly indicated in figure 11 which presents the variation of side force with drift angle for constant values of vertical force. The data are widely scattered in many cases; however, the trend would seem to be similar to that shown by the faired curves presented in figure 11. In the low range of vertical force (curves a, b, c, d), the side force increases with increasing vertical force at a given drift angle. At higher vertical forces (curves e, f, g, h) the side force tends to become independent of vertical force and to vary primarily with drift angle.

CONCLUSIONS

This paper has presented some results obtained from tests conducted on a large bomber-type airplane to determine the ground-reaction forces imposed on the main landing gear under actual landing conditions. The test program covered 30 landings made at vertical velocities up to 8.4 feet per second and forward ground speeds from 81.0 to 119.5 knots on both wet and dry concrete runways. A summary of some of the principal results follows:

(1) The vertical force on the truck at which the oleopneumatic shock strut begins to compress varies over a wide range. The shock-strut motion did not start at the beginning of the impact but was delayed until the vertical force on the truck had reached values ranging from 9,000 to 45,500 pounds. There was apparently no relation between this breakout force and any other force or condition of the impact.

(2) The computed variation of maximum vertical force with vertical velocity agreed reasonably well with the experimental results.

(3) There was a frequent occurrence of unsymmetrical vertical forces on the two wheels of a truck resulting in unsymmetrical drag forces, particularly during the time when one wheel had spun up and the other was still in the process of spinning up.

(4) The mean value of coefficient of friction for the dry runway increased gradually from a value of 0.40 at the beginning of spin-up (slip ratio of 0.90) to a maximum value of 0.72 at a slip ratio of 0.13. The mean value of coefficient of friction for the wet runway varied from

0.20 at the beginning of spin-up to a maximum value of 0.41 at a slip ratio of 0.07.

(5) In the low vertical-force range, the side force varied with drift angle and vertical force. At high vertical forces, side force varied primarily with drift angle and further increase of vertical force had little effect on side force at a given drift angle.

Langley Aeronautical Laboratory,
National Advisory Committee for Aeronautics,
Langley Field, Va., February 6, 1958.

APPENDIX

METHOD OF COMPUTING SPIN-UP AND SPRING-BACK DRAG FORCES IN AN UNSYMMETRICAL LANDING IMPACT OF A DUAL-WHEEL LANDING-GEAR TRUCK

In this appendix the method used to calculate the dynamic forces and moments presented in figures 9 and 10, respectively, for landing 15 is discussed. The method makes use of the measured time histories of the vertical force and an approximation of the mean variation of coefficient of friction with slip ratio shown in figure 8(b). A sketch of the simplified dual-wheel landing-gear configuration with the notation used in the calculations is presented in figure 12.

The forward and rearward displacement of the truck due to bending was assumed to be proportional to the total drag force at the axle; the twisting of the truck was likewise assumed to be proportional to the yawing moment and to take place entirely about the vertical center line of the truck (no offset being assumed between the axle center line and the strut center line). The velocity of the airplane and the rolling radius for each tire was assumed to be constant throughout the impact.

The slip ratio S is defined in reference 5 as

$$S = \frac{V_{axle} - r_r\dot{\theta}}{V_{axle}}$$

where

V_{axle} velocity of axle

r_r rolling radius of wheel

$\dot{\theta}$ angular velocity of wheel under application of torque

The axle velocity may be expressed as

$$V_{axle} = V_a - \dot{\delta}$$

where

V_a airplane velocity

δ axle displacement due to flexibility of landing gear (positive when rearward)

The slip ratio then becomes

$$S = \frac{V_a - \dot{\delta} - r_r\dot{\theta}}{V_a - \dot{\delta}}$$

The $\dot{\delta}$ term was eliminated from the denominator since $\dot{\delta}$ was small compared with V_a; however, in the numerator $\dot{\delta}$ was retained since it was significant compared with $V_a - r_r\dot{\theta}$. The equation used for slip ratio in these computations is

$$S = \frac{V_a - \dot{\delta} - r_r\dot{\theta}}{V_a} \tag{1}$$

Four degrees of freedom for the truck were assumed: forward and rearward bending in the strut, twisting about the strut axis, and rotation of each wheel. The equation of motion for forward and rearward bending is

$$\ddot{\delta}_R + \ddot{\delta}_L + \omega_X^2\left(\delta_R + \delta_L\right) = \frac{F_{h,R} + F_{h,L}}{m} \tag{2}$$

where

ω_X natural frequency of gear in forward and rearward bending

m mass of each wheel and tire

R, L subscripts denoting right and left wheels, respectively, of truck (for this case R is for right outboard and L is for right inboard)

The equation of motion for twisting is

$$\ddot{\delta}_R - \ddot{\delta}_L + \omega_Z^2\left(\delta_R - \delta_L\right) = \left(F_{h,R} - F_{h,L}\right)\frac{c^2}{2I_Z} \tag{3}$$

where

ω_Z natural frequency of gear in torsion

I_Z moment of inertia of wheels about vertical center line of truck

C distance between the two wheels of a truck

If the vertical force is assumed to act through the axle center line, the equation of rotation for each wheel is

$$\ddot{\theta} = \frac{F_h r_d}{I_\theta} = \frac{F_v \mu r_d}{I_\theta} \tag{4}$$

where

r_d distance from axle to ground

I_θ moment of inertia of wheel about axle

If it is assumed that V_a and r_r are constant, differentiating equation (1) with respect to time gives

$$\dot{s} = -\frac{\ddot{\delta}}{V_a} - \frac{\ddot{\theta} r_r}{V_a}$$

Substituting equation (4) into this expression gives

$$\dot{s} = -\frac{\ddot{\delta}}{V_a} - \frac{F_v r_d r_r}{I_\theta V_a} \mu \tag{5}$$

The resulting equations of motion for the system are

$$\left.\begin{aligned}
&\ddot{\delta}_R + \ddot{\delta}_L + \omega_X^2\left(\delta_R + \delta_L\right) - \frac{F_{v,R}}{m}\mu_R - \frac{F_{v,L}}{m}\mu_L = 0 \\
&\ddot{\delta}_R - \ddot{\delta}_L + \omega_Z^2\left(\delta_R - \delta_L\right) - \frac{F_{v,R}c^2}{2I_Z}\mu_R + \frac{F_{v,L}c^2}{2I_Z}\mu_L = 0 \\
&\frac{\ddot{\delta}_R}{V_a} + \frac{F_{v,R}r_d r_r}{I_\theta V_a}\mu_R + \dot{s}_R = 0 \\
&\frac{\ddot{\delta}_L}{V_a} + \frac{F_{v,L}r_d r_r}{I_\theta V_a}\mu_L + \dot{s}_L = 0
\end{aligned}\right\} \qquad (6)$$

For these computations the variation of μ with S was approximated by two straight lines as follows: For $S = -0.13$ to 0.13, μ varied linearly from -0.73 to 0.73 or

$$\mu = 5.62S \qquad (-0.13 < S < 0.13) \qquad (7)$$

and for $S = 0.13$ to 1.00, μ varied from 0.73 to 0.45 or

$$\mu = 0.77 - 0.32S \qquad (0.13 < S < 1.00) \qquad (8)$$

In order to obtain the drag forces, the computations were divided into three intervals: the first was the interval in which both wheels were operating at slip ratios greater than 0.13, the second was that interval in which one wheel (the left in this case) was operating at slip ratios less than 0.13 while the other wheel was still operating at slip ratios greater than 0.13, and the third was the interval in which both wheels were operating at slip ratios less than 0.13. By substituting the proper variation of μ_R and μ_L (eqs. (7) and (8)) for each of the three intervals, equations (6) can be solved and the variation of the slip ratio with time can be determined. By substituting these values of slip ratio into equations (7) and (8) and using the relation $F_h = \mu F_v$, the variation of drag force with time can be determined.

In computing the drag forces shown in figure 9 certain simplifications were made. Since the flexibility of the gear has a relatively small effect on the slip ratio, this flexibility would have very little effect on F_h in the first interval because of the insignificant variations of μ with these small variations of S. Therefore, equation (5)

was modified by eliminating the $\ddot{\delta}$ term and solved separately for each wheel by a simple iteration process from the initial condition of $S = 1.00$ until one of the wheels reached a slip ratio of 0.13 (in this case the left wheel). This solution gave values of S for time increments throughout this interval. By use of this time history of S the time history of F_h was determined for both wheels. Equations (2) and (3) were evaluated for small time intervals, $\Delta t = 0.01$ second, assuming that $\left(F_{h,R} + F_{h,L}\right)$ and $\left(F_{h,R} - F_{h,L}\right)$ varied linearly with time during these small intervals. From these results variations of δ_R, δ_L, S_R, and S_L with time were determined and from these time histories the initial conditions for the second interval were obtained.

During the second interval the vertical forces were reaching a peak and the variation with time was much less than in the first interval, so that for each wheel a constant value of F_V equal to the average F_V of that wheel during the interval was assumed. Equations (7) and (8) were substituted for μ_L and μ_R, respectively, in equations (6) and simultaneous solutions up to the time that $S_R = 0.13$ gave time histories of δ_R, δ_L, S_R, and S_L. These time histories established the initial conditions for the third interval and the slip-ratio time histories established the drag-force variation of each wheel for the second interval.

The third interval was computed in the same manner as the second interval except that equation (7) was substituted for both μ_L and μ_R in equations (6).

For computing the bending moment in the axle, the following relation was used for the right side (see fig. 12):

$$M_{h,R} = F_{h,R}B_R - mB_R\ddot{\delta}_R - I_\omega\left(\frac{\ddot{\delta}_R - \ddot{\delta}_L}{C}\right) \tag{9}$$

where

$M_{h,R}$ bending moment in axle (at station 2 shown in fig. 3)

B_R distance from center of wheel to station 2

I_ω moment of inertia of wheel about its vertical axis

Similarly, for the left axle

$$M_{h,L} = F_{h,L}B_L - mB_L\ddot{\delta}_L - I_\omega\left(\frac{\ddot{\delta}_L - \ddot{\delta}_R}{C}\right) \tag{10}$$

It may be seen that the moment in the left axle produced by a positive drag force is of opposite sign to that produced in the right axle by a positive force. In presenting the data in figure 10, however, the moment produced by a positive drag force was presented as a positive moment for either axle.

REFERENCES

1. Dreher, Robert C.: An Airborne Indicator for Measuring Vertical Velocity of Airplanes at Wheel Contact. NACA TN 2906, 1953.

2. Horne, Walter B.: Static Force-Deflection Characteristics of Six Aircraft Tires Under Combined Loading. NACA TN 2926, 1953.

3. Theisen, Jerome G., and Edge, Philip M., Jr.: An Evaluation of an Accelerometer Method for Obtaining Landing-Gear Drag Loads. NACA TN 3247, 1954.

4. Milwitzky, Benjamin, and Cook, Francis E.: Analysis of Landing-Gear Behavior. NACA Rep. 1154, 1953. (Supersedes NACA TN 2755.)

5. Milwitzky, Benjamin, Lindquist, Dean C., and Potter, Dexter M.: An Experimental Study of Applied Ground Loads in Landing. NACA Rep. 1248, 1955. (Supersedes NACA TN 3246.)

TABLE I.- SUMMARY OF TEST CONDITIONS AND MEASURED FORCES

Landing	Gross weight, lb	Time of impact of landing gear, sec			Vertical velocity of landing gear, fps			Maximum total F_V on truck, lb		Shock-strut breakout force on truck, lb		Maximum F_V on wheel, lb		Maximum F_h on wheel, lb		Runway condition
		Left	Right	Nose	Left	Right	Nose	Left	Right	Left	Right	Left outboard	Right outboard	Left outboard	Right outboard	
1	97,780	0	0.27	4.09	2.65	1.60	1.00	27.4×10^3	17.2×10^3	29.4×10^3	(b)	15.8×10^3	8.4×10^3	6.8×10^3	3.4×10^3	Dry
2	97,340	0	1.30	1.54	1.30	1.50	2.20	14.1	24.5	(b)	23.8×10^3	9.5	9.7	5.8	4.9	
3	96,940	0	.94	3.98	1.90	1.65	.30	22.8	20.5	22.4	20.4	16.4	8.6	10.2	5.4	
4	96,250	.53	3.92	0	1.10	.65	.95	20.2	20.5	18.5	19.8	11.8	8.7	7.0	4.4	
5	95,770	0	.16	2.23	2.35	1.65	1.25	22.5	21.0	9.0	21.0	13.0	6.4	7.5	3.6	
6	95,290	0	.96	.90	1.75	.30	.95	20.7	18.6	18.6	17.0	13.9	8.5	7.2	5.6	
7	98,690	0	.48	.50	1.75	1.00	1.20	28.7	11.8	26.5	(b)	16.5	5.2	8.5	3.4	
8	98,160	0	1.06	.54	1.30	.60	2.00	19.0	12.3	(b)	(b)	10.7	6.8	6.3	4.8	
9	97,660	0	3.80	.71	2.90	.60	1.10	24.2	16.1	20.5	(b)	17.5	5.5	11.1	3.4	
10	97,010	0	1.41	.23	3.85	.35	2.35	29.0	18.4	25.0	18.3	20.5	7.6	9.8	4.2	
11	96,480	.24	.38	0	3.20	2.90	2.65	25.6	20.0	25.0	19.8	14.2	5.0	8.2	3.5	
12	95,970	0	.19	.16	2.80	2.35	2.35	29.0	23.2	23.0	22.0	17.4	6.0	10.3	3.2	
13	99,430	0	.02	5.33	5.55	5.40	.65	59.4	53.5	32.0	31.2	29.9	21.5	18.6	14.0	
14	99,080	0	1.70	6.97	6.45	.70	.35	(a)	19.3	31.6	(b)	(a)	7.6	22.9	5.4	
15	98,730	0	.01	2.17	6.25	6.10	.65	65.0	(a)	28.0	21.2	30.9	24.5	20.0	17.3	
16	98,200	0	.04	2.60	3.90	3.60	.80	31.6	28.1	28.3	25.2	16.0	10.8	10.7	7.4	
17	97,850	.10	0	4.95	5.75	7.15	1.00	39.7	(a)	33.0	41.2	16.0	36.0	12.0	18.5	
18	97,470	0	.14	.78	8.40	5.70	.95	73.6	42.3	45.5	25.2	39.8	20.0	23.3	12.0	
19	119,580	0	.12	----	3.05	2.70	----	(a)	29.2	34.7	23.0	27.0	11.4	----------	6.8	
20	118,760	0	1.12	----	1.15	1.05	----	25.3	27.4	(b)	25.6	16.0	10.7	----------	6.8	
21	118,190	0	.16	----	4.35	3.10	----	50.4	31.7	33.3	36.1	24.7	12.8	----------	8.4	
22	117,700	0	.38	----	2.90	.90	----	31.6	11.8	28.5	(b)	15.4	5.0	----------	3.6	
23	117,130	0	.04	----	2.15	2.60	----	31.6	23.0	27.4	27.2	11.6	11.1	----------	7.7	
24	116,630	0	.06	----	3.15	2.90	----	35.4	31.0	32.6	29.5	16.2	13.0	----------	6.8	
25	96,230	0	.04	----	3.70	3.80	----	34.5	35.0	27.5	31.2	16.8	13.7	5.6	3.8	Wet
26	95,600	0	.21	----	4.95	4.20	----	41.6	34.4	27.5	33.7	23.5	12.0	8.4	5.2	
27	95,540	0	.045	----	4.95	4.60	----	31.7	46.5	20.5	36.3	26.2	16.6	12.5	4.7	
28	95,150	0	.17	----	2.60	2.25	----	36.6	29.0	23.6	27.8	16.4	12.0	4.2	3.6	
29	94,870	0	.54	----	3.30	1.00	----	42.6	22.0	28.7	(b)	25.6	9.6	6.0	4.2	
30	94,580	0	.58	----	1.50	1.45	----	27.7	25.6	22.0	(b)	17.2	10.2	7.8	3.4	

[a]Exceeds strain-gage calibration range.

[b]Shock strut did not compress during impact.

TABLE II.- INITIAL IMPACT CONDITIONS

Landing	c.g. acceleration, g units	Roll attitude, deg	Roll velocity, radians/sec	Pitch attitude, deg	Pitch velocity, radians/sec	Drift angle, deg	Ground speed, knots
1	0.97	-1.2	-0.010	2.6	0.020	----	84.0
2	1.08	-1.3	0	4.8	.015	-1.0	81.0
3	1.04	-2.2	0	4.2	.010	-2.0	83.1
4	1.00	-2.3	.010	.2	-.005	----	91.6
5	.98	-.8	-.005	2.6	.025	-1.5	102.3
6	.99	-1.6	0	2.0	.020	----	103.9
7	.95	-1.6	-.005	3.2	-.020	----	82.5
8	1.02	-1.6	-.010	3.0	-.020	8.5	84.0
9	1.11	-2.6	-.020	3.2	-.005	2.0	86.7
10	1.01	-2.9	-.005	2.5	.010	4.4	106.8
11	.98	-1.0	.010	.1	.015	----	109.4
12	1.00	-1.2	0	2.0	0	2.5	102.3
13	1.05	-.4	0	5.2	.055	----	85.3
14	1.10	-1.6	-.030	7.8	.040	1.6	89.5
15	1.02	-.3	-.015	6.5	.030	-2.6	86.7
16	1.09	-.3	-.005	4.6	-.015	.9	96.0
17	.94	1.2	.025	7.6	-.010	-1.8	103.9
18	1.06	-2.2	-.010	8.8	.025	-2.6	101.0
19	.99	-.8	0	3.2	.020	----	102.5
20	1.03	-2.2	.005	4.4	.010	-.4	92.5
21	1.04	-1.1	-.010	5.7	.035	0	91.7
22	1.06	-1.6	0	7.3	.025	0	105.2
23	.98	-.4	.015	6.7	.010	----	101.0
24	1.00	-.3	.005	6.6	.005	----	103.9
25	.96	0	0	1.9	.015	----	87.5
26	.97	-1.7	.005	2.1	.050	1.0	89.4
27	1.01	-.3	0	2.2	.025	3.3	88.2
28	.94	-.8	.005	3.7	-.010	-.3	96.6
29	.99	-2.2	-.010	2.4	0	-1.1	99.5
30	.94	-2.0	.015	2.0	-.040	1.4	98.9

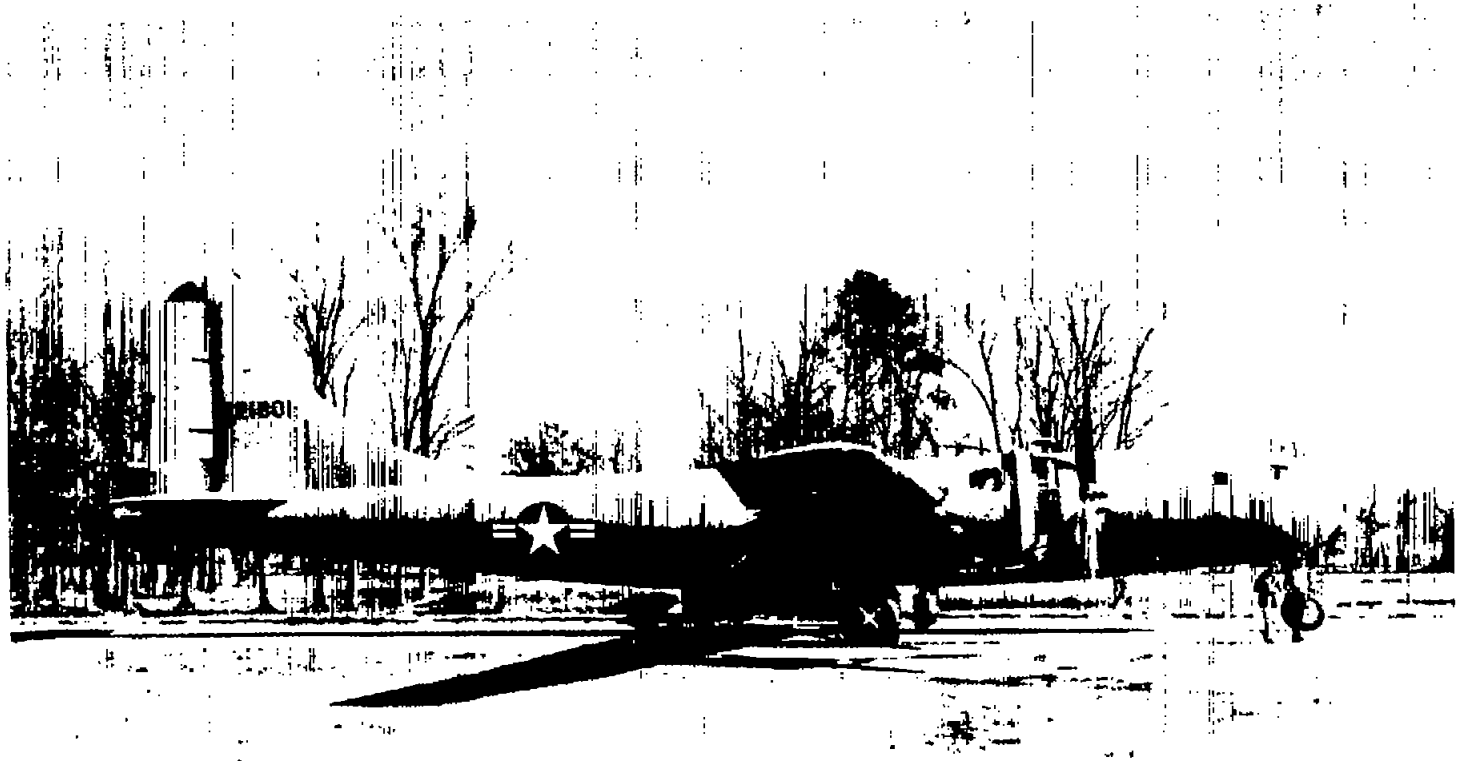

Figure 1.- Airplane used in the investigation. L-78020

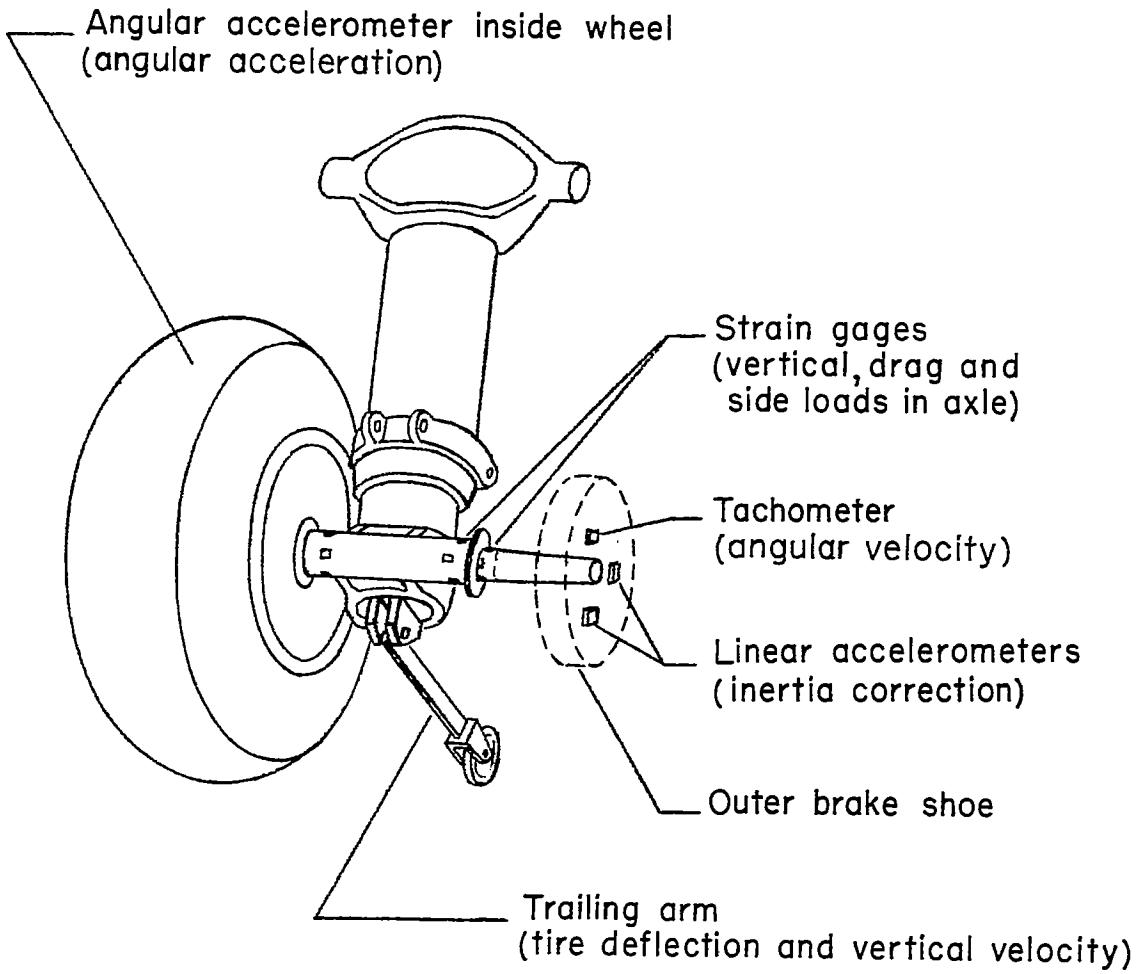

Figure 2.- Main landing-gear truck with one wheel removed to show arrangement of instrumentation. Trailing arm also shown.

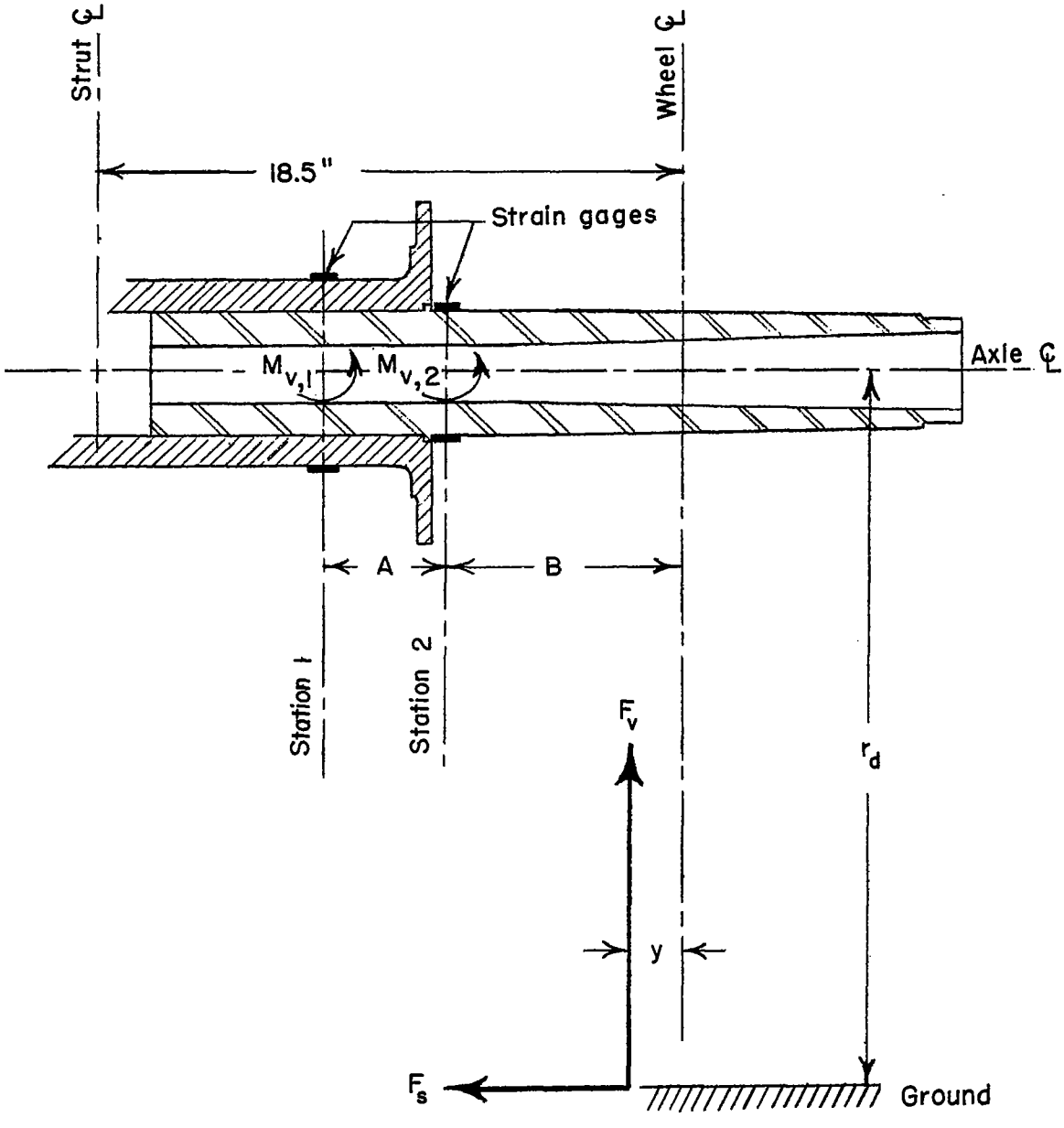

Figure 3.- Vertical section of axle structure.

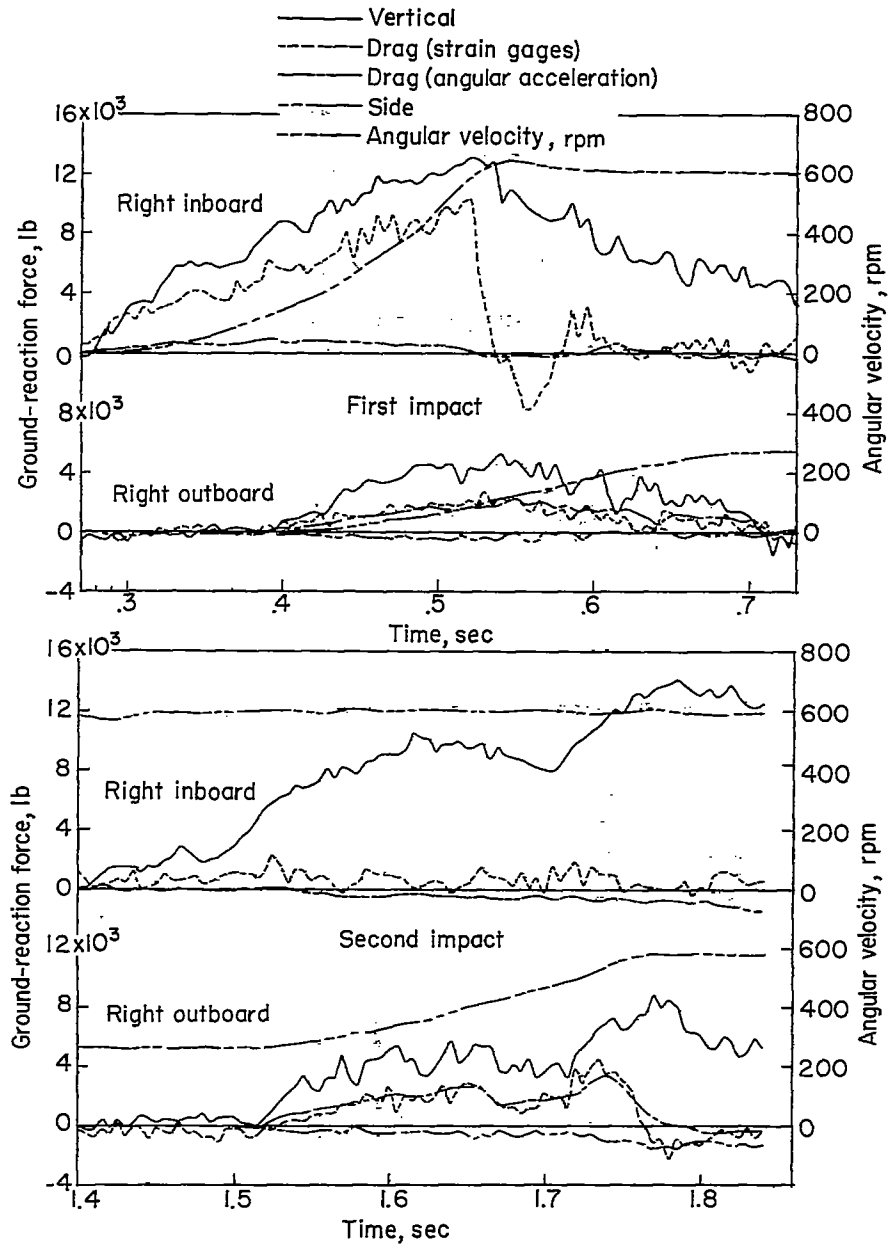

(a) Dry runway, V_V = 1.60 fps (first impact), V_V = 0.25 fps (second impact), landing 1.

Figure 4.- Typical time histories of ground-reaction forces and wheel angular velocities for several impacts.

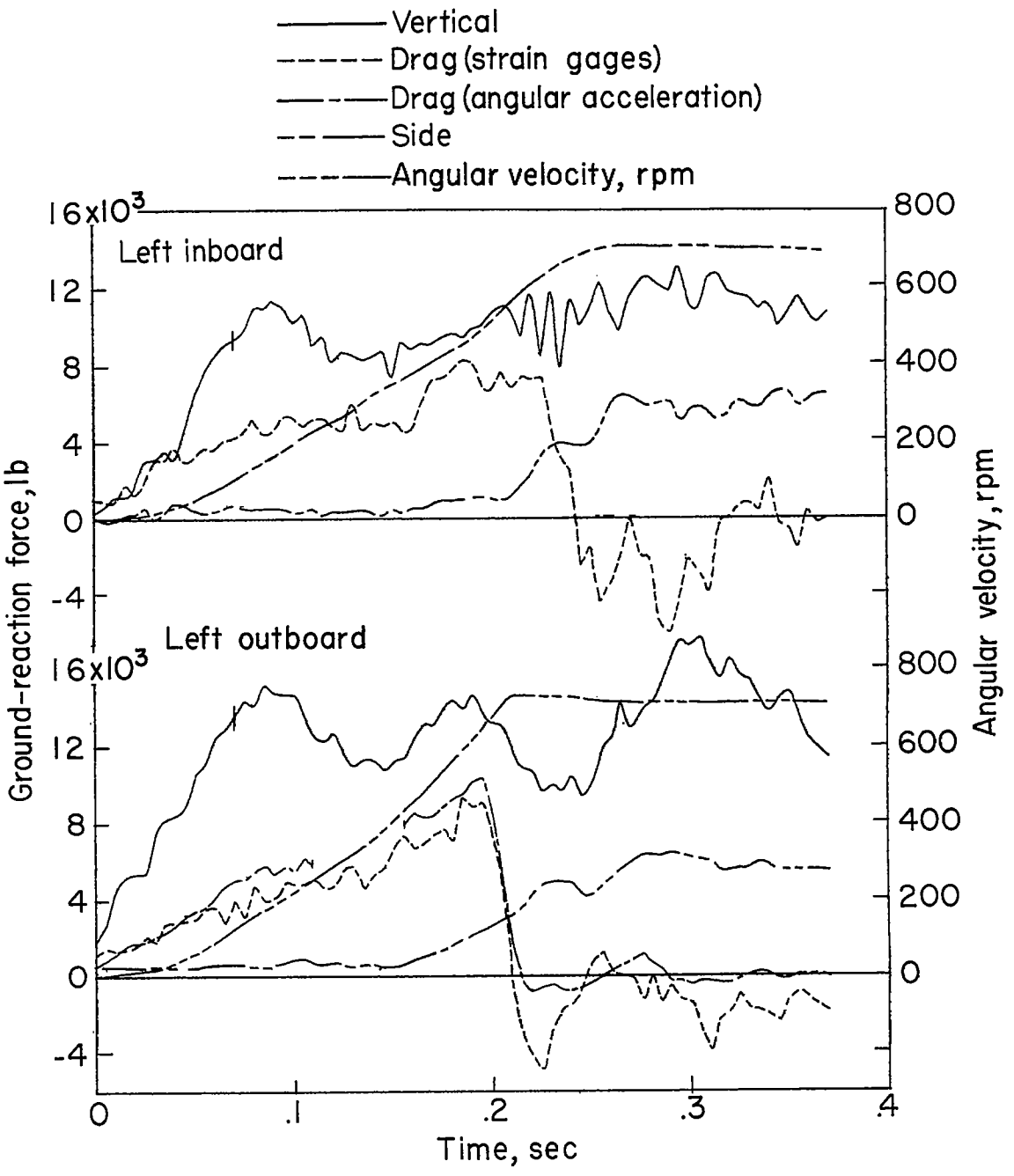

(b) Dry runway, V_V = 2.80 fps, landing 12. Ticks on vertical-force curves indicate point at which shock strut begins to compress.

Figure 4.- Continued.

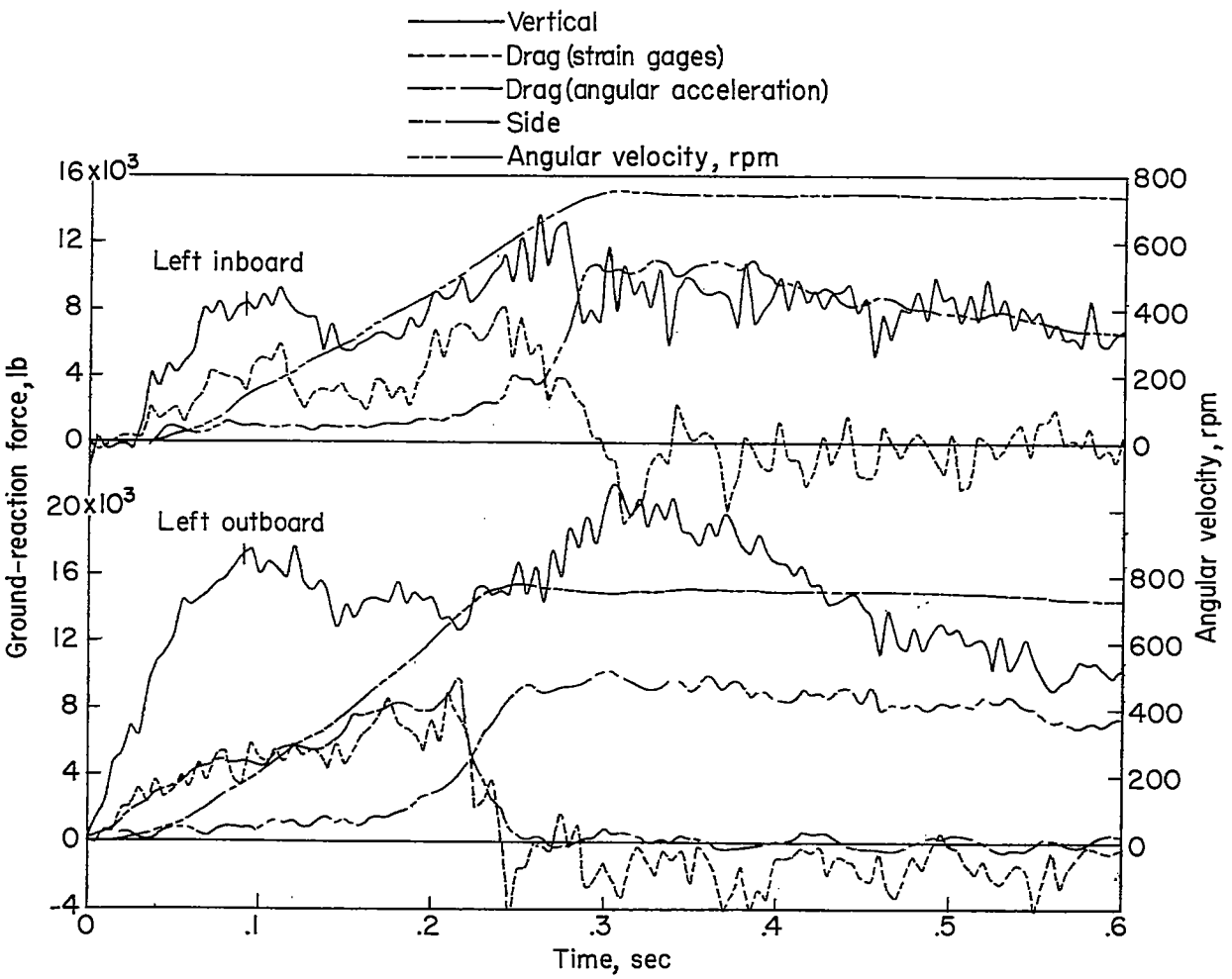

(c) Dry runway, V_V = 3.85 fps, landing 10. Ticks on vertical-force curves indicate point at which shock strut begins to compress.

Figure 4.- Continued.

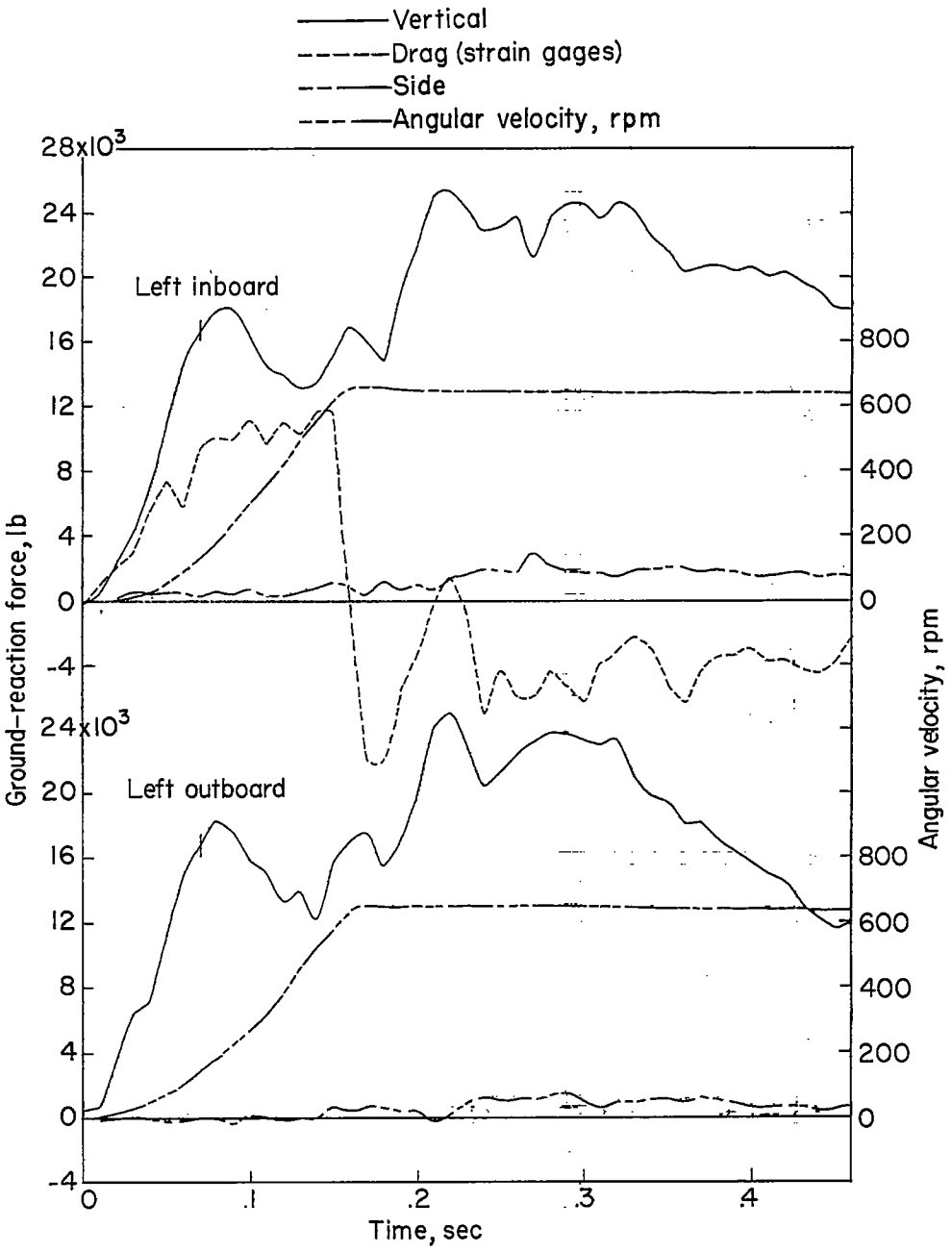

(d) Dry runway, V_V = 4.35 fps, landing 21. Ticks on vertical-force curves indicate point at which shock strut begins to compress.

Figure 4.- Continued.

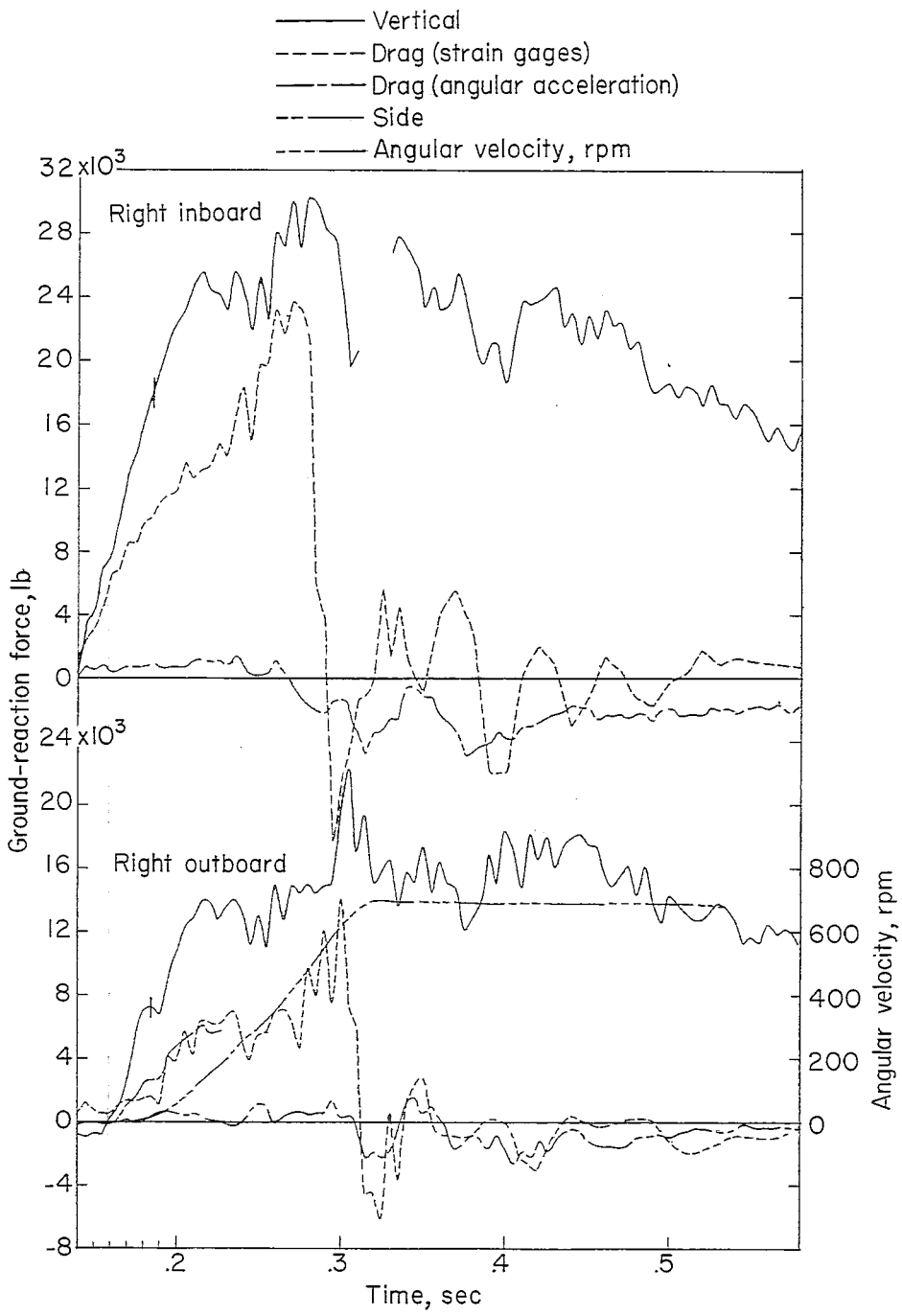

(e) Dry runway, V_V = 5.70 fps, landing 18. Ticks on vertical-force curves indicate point at which shock strut begins to compress.

Figure 4.- Continued.

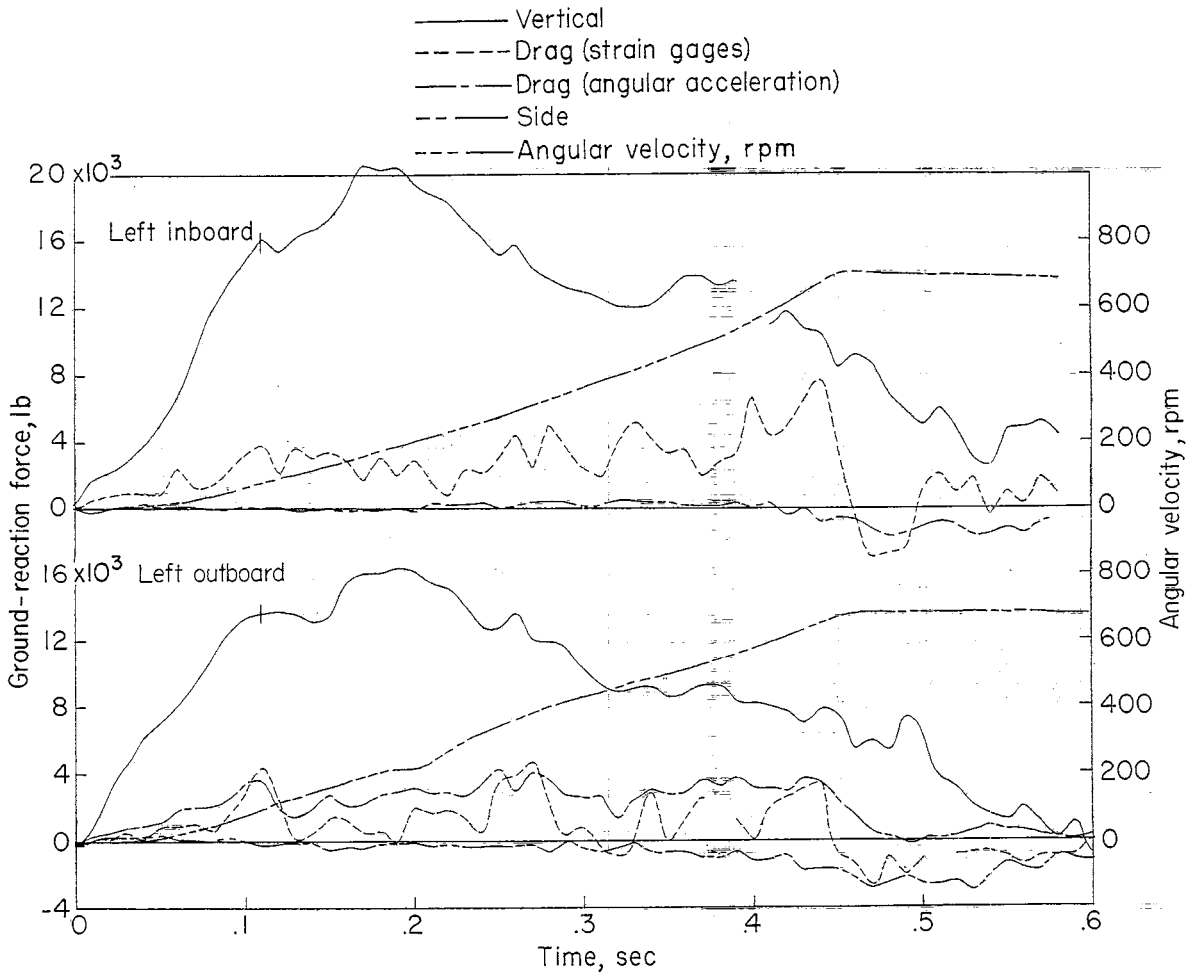

(f) Wet runway, V_v = 2.60 fps, landing 28. Ticks on vertical-force curves indicate point at which shock strut begins to compress.

Figure 4.- Concluded.

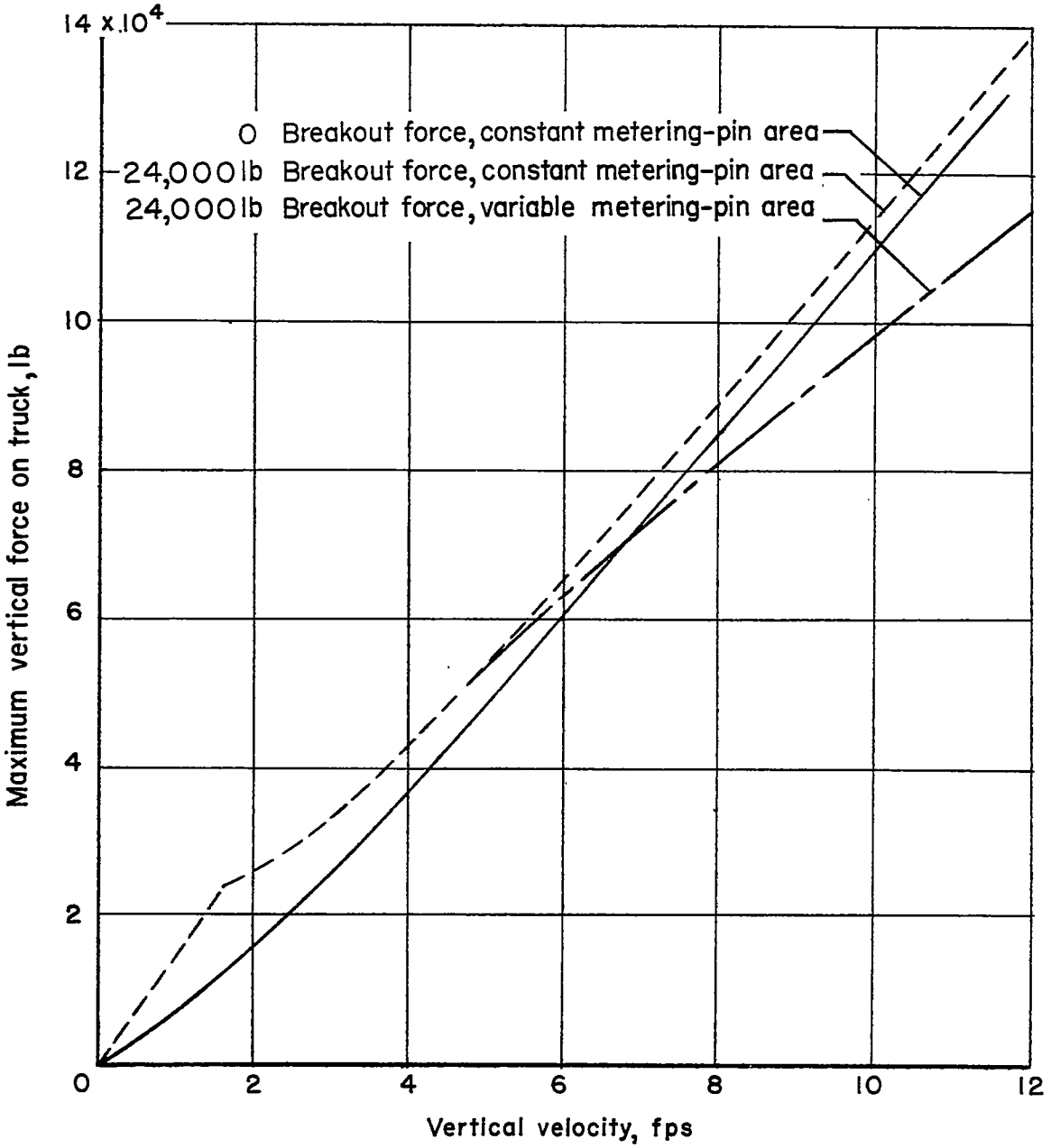

Figure 5.- Calculated variation of maximum truck vertical force with vertical velocity.

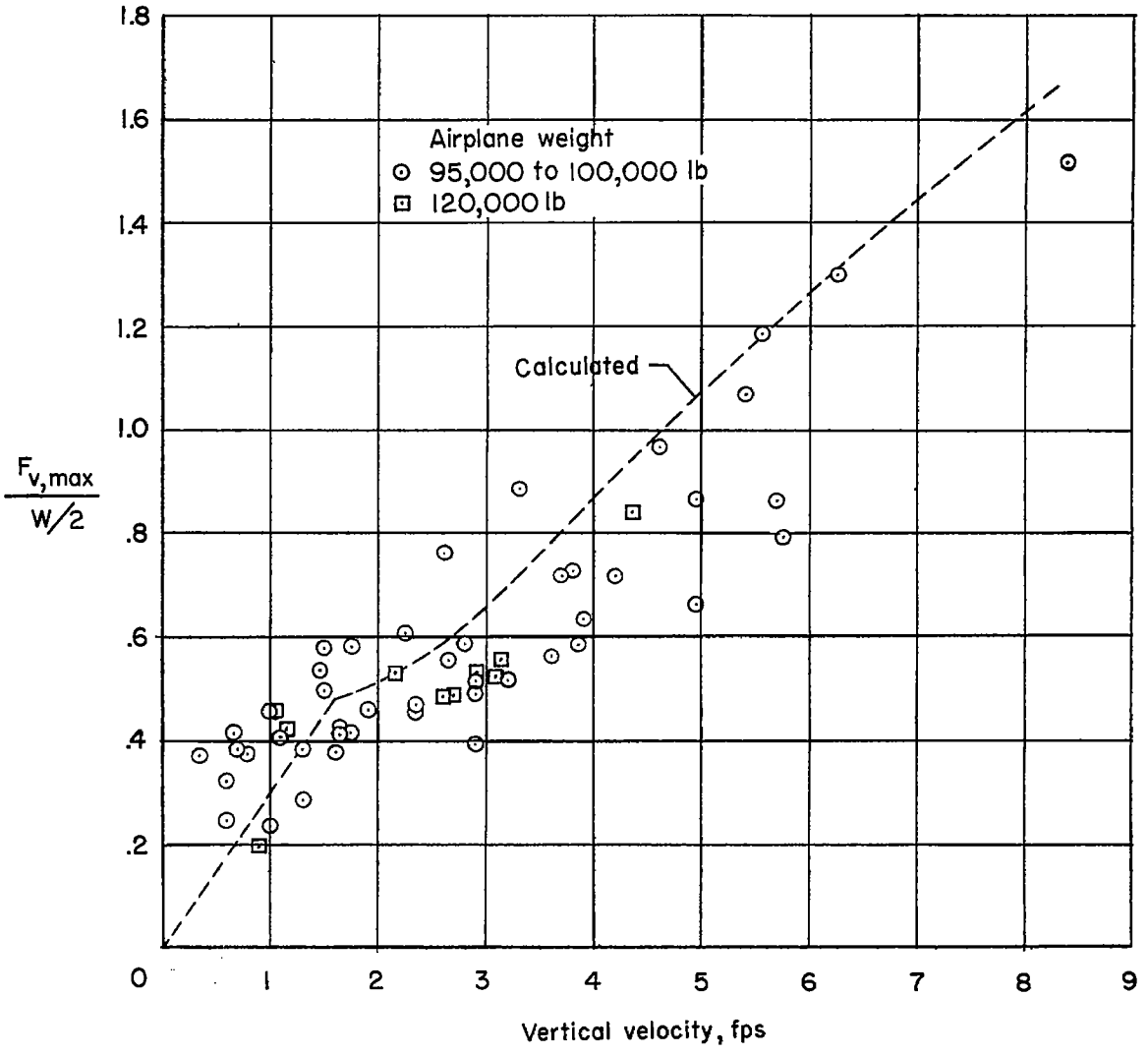

Figure 6.- Variation with vertical velocity of maximum truck vertical force divided by one-half of the airplane weight.

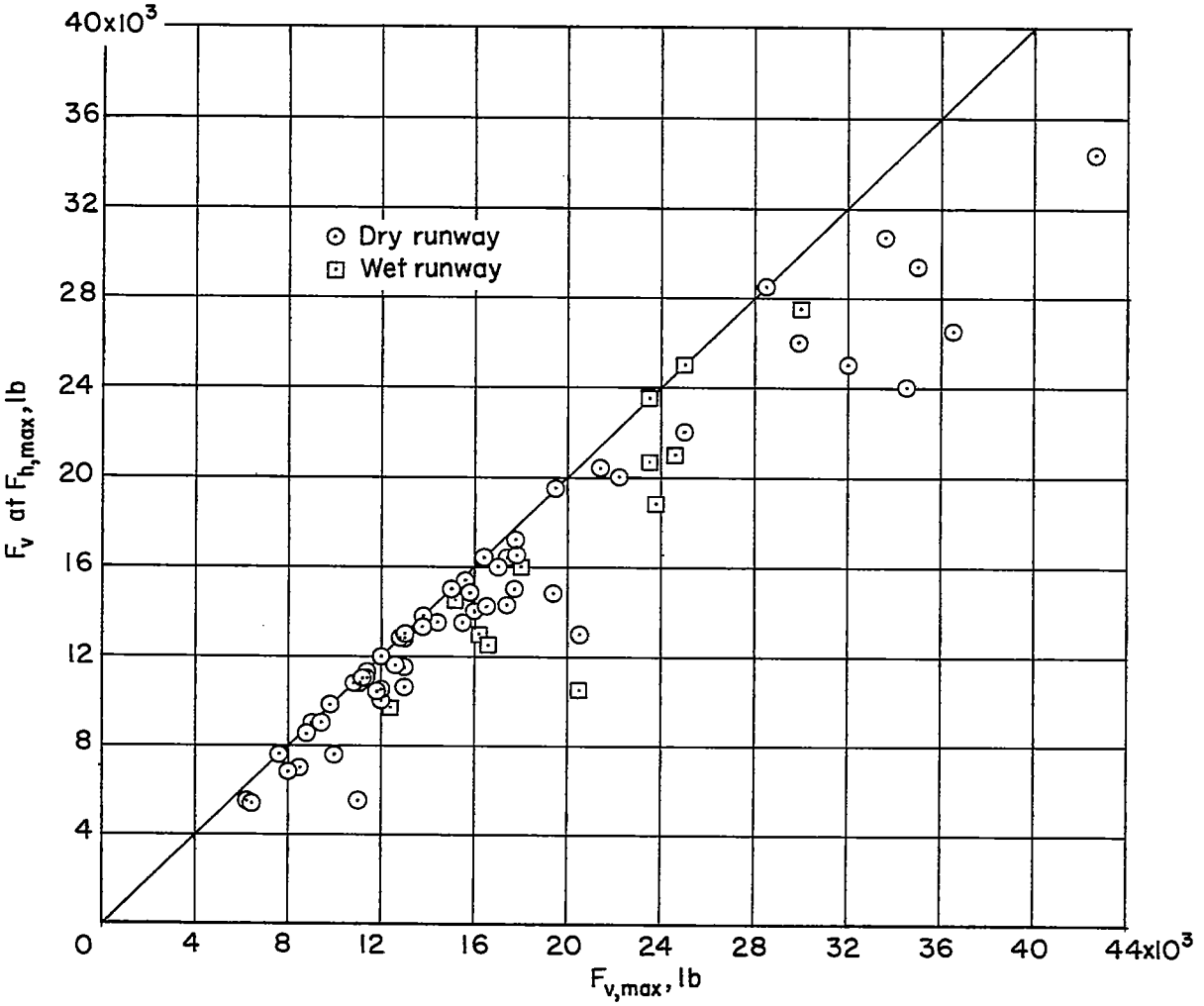

Figure 7.- Variation of F_v at $F_{h,max}$ with $F_{v,max}$ for each impact.

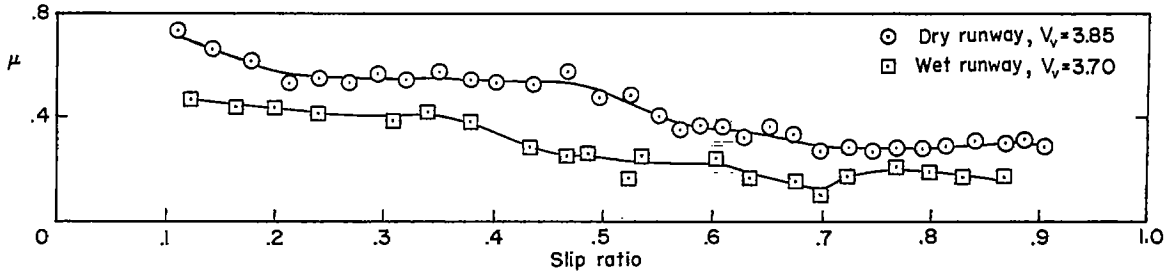

(a) Sample data from two typical impacts.

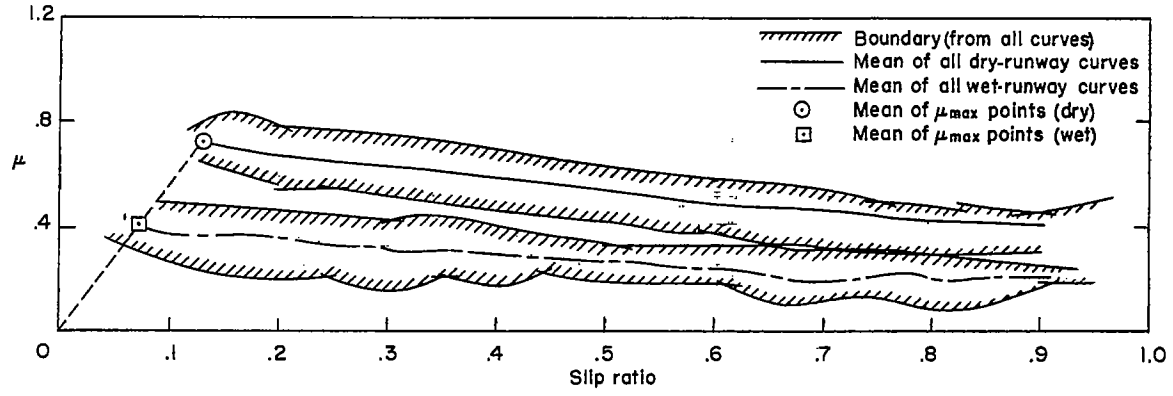

(b) Data from all impacts.

Figure 8.- Variation of coefficient of friction with slip ratio.

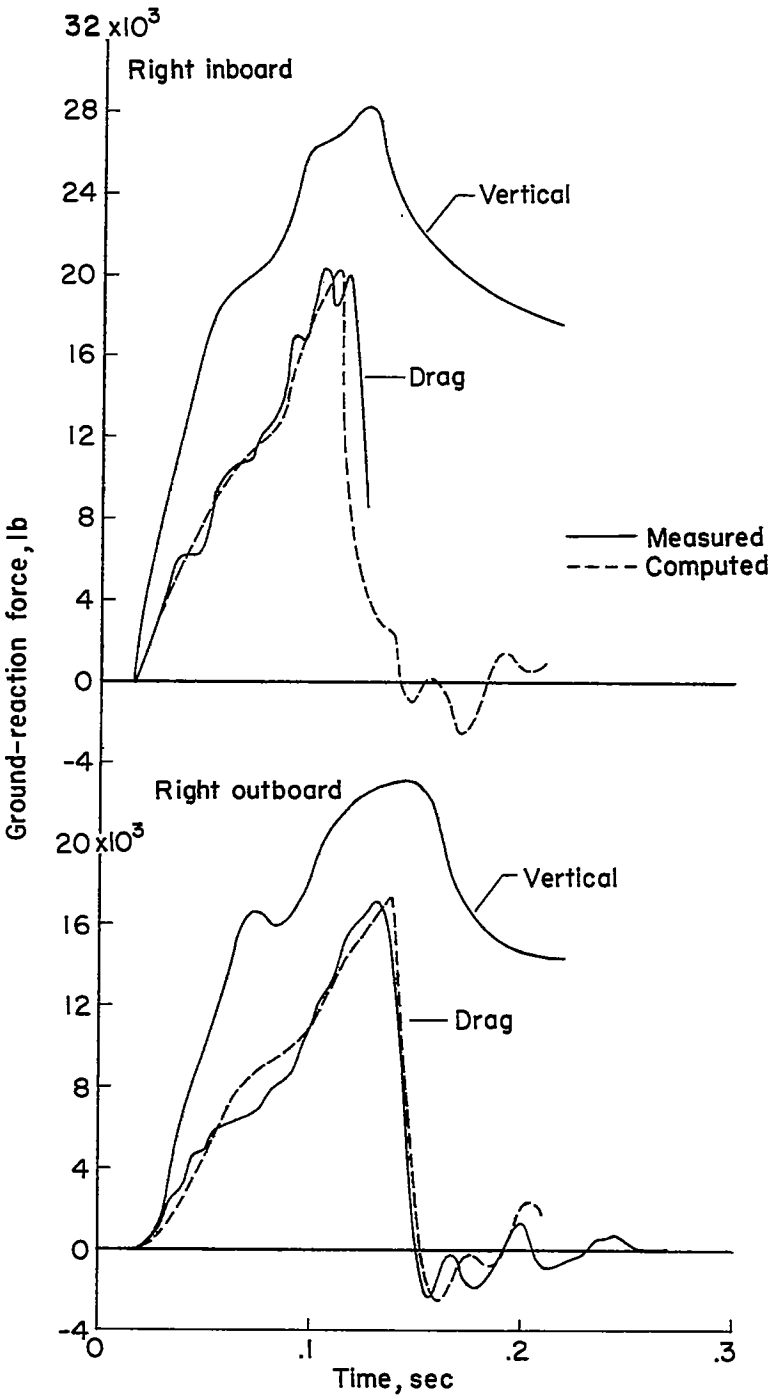

Figure 9.- Comparison of computed and measured ground-reaction drag forces. Dry runway, V_V = 6.10 fps, landing 15.

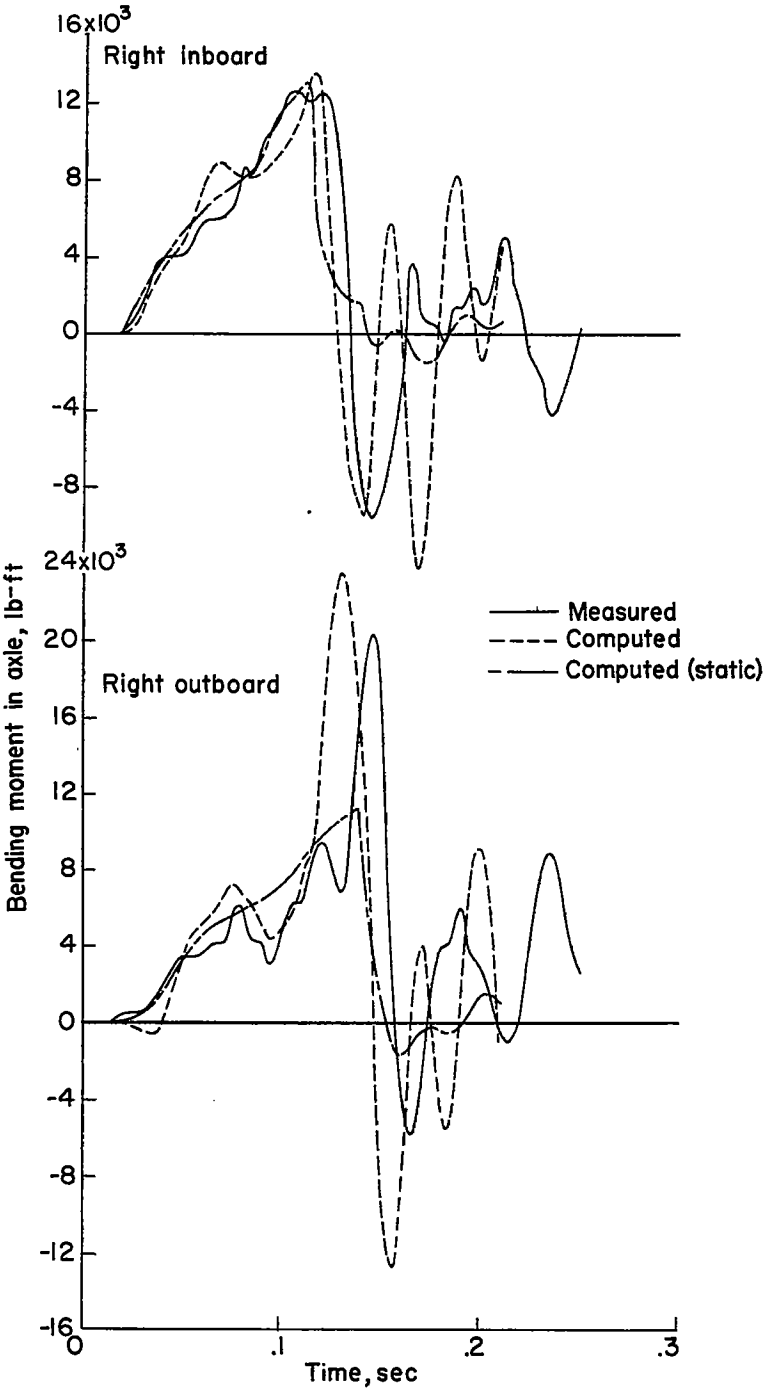

Figure 10.- Comparison of computed and measured bending moment in axles. Dry runway, V_V = 6.10 fps, landing 15.

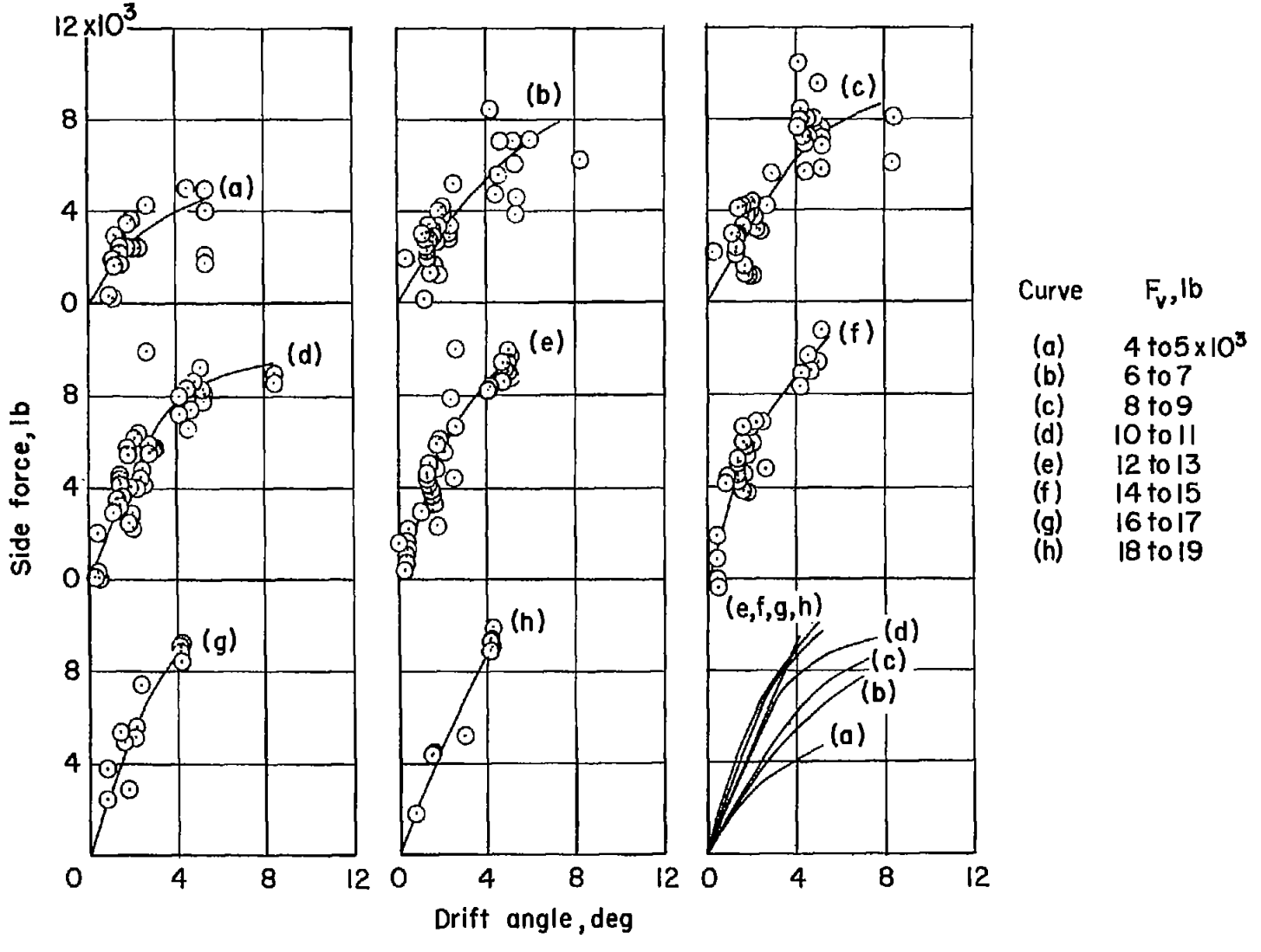

Figure 11.- Side-force variation with drift angle for constant values of vertical force.

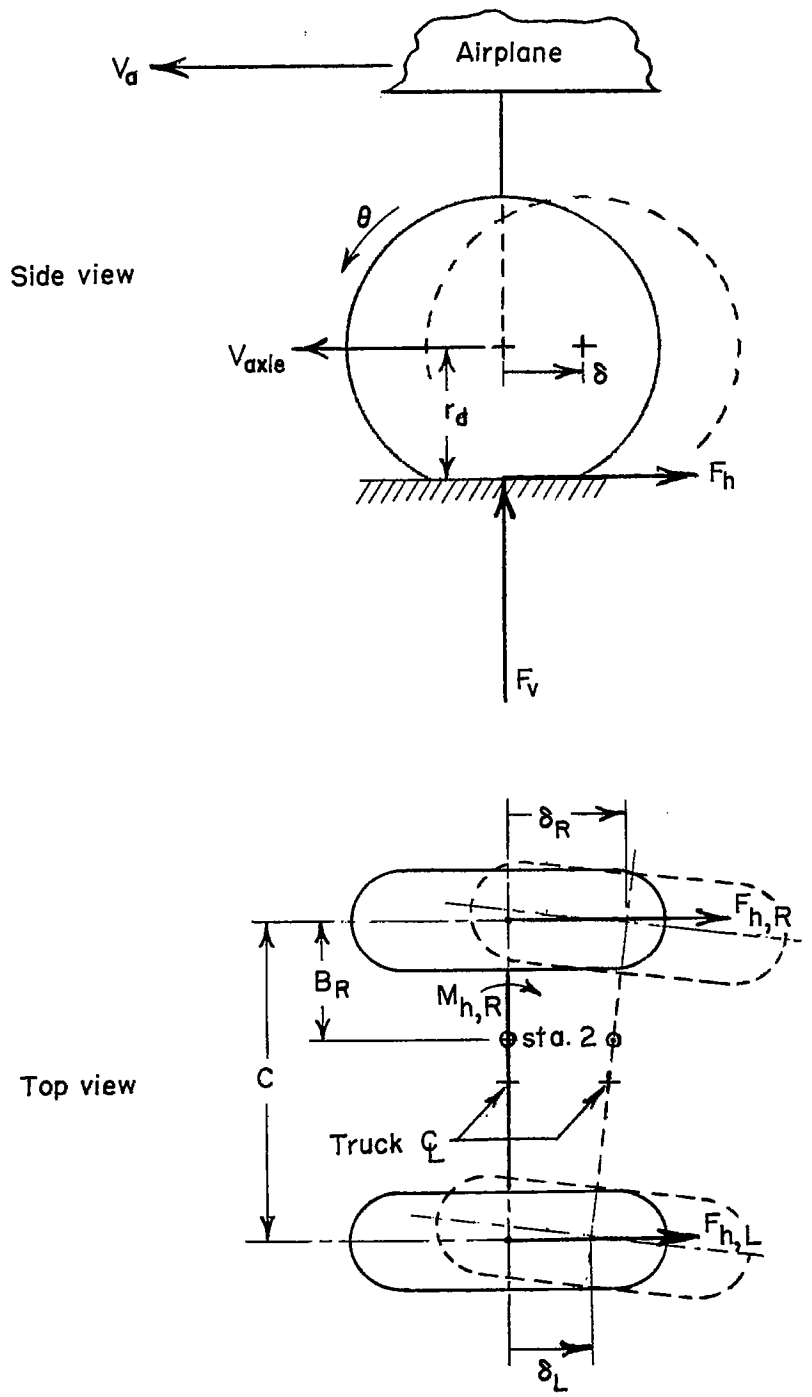

Figure 12.- Simplified dual-wheel landing-gear configuration used in the drag-force and axle-bending-moment computations.